Supporting Information for

"The role of tides in ocean–ice-shelf interactions in the southwestern Weddell Sea"

U. Hausmann[1], et al.

[1]Sorbonne-Université, LOCEAN-IPSL, Paris, France

Contents

1. Note S1
2. Figures S1 to S3
3. Table S1

Introduction

This supporting information provides further characterization of the water-mass properties of the reference simulation, for different open-ocean regions and cavities (Figs. S1 and S2, respectively), as well as a characterization of the water-mass changes induced by the presence of tides (Fig. S3), with further discussion of these provided in Supplementary Note S1. Furthermore Table S1 provides additional details on ocean model parameterizations used.

Note S1. Water mass properties and impact of tides

Further characterization (in addition to Fig. 5 & 6) of the reference simulation's volume census in conservative temperature (Θ)-absolute salinity (S_A) space for several subdomains of the regional simulation is provided in Figs. S1 & S2.

Open-ocean water masses Water mass distributions for open-ocean gyre and continental shelf regions (cf. map in Fig. S1d) are color-contoured in Fig. S1 (panels S1a & b show the southwestern & southeastern deep open ocean, panels c, e & f the northwestern, southwestern, eastern continental shelves; here panel S1e is repeated from Fig. 5b to place it in the regional context). As in Fig. 5, the gray dots superimposed on the model volumetric Θ-S_A contours represent observed Θ-S_A from all available in-situ profiles acquired by ships, Argo floats and instrumented seals, within each of the regions post 1972, with profile locations mapped and counted in panel Fig. S1d. Profiles are obtained through all seasons, with the summer-focus of ship observations mediated by the addition of seals, as well as of Argo floats, including under sea ice (with interpolated coordinates as seen in Fig. S1d). Note that in-situ profiles represent the respective instantaneous local ocean state as indication of observed water-mass populations, rather than a quantitative census of volume distributions as available in the model. Overall this comparison shows that water masses observed coincide with the primary poles of simulated water masses in each of the open-ocean regions considered. In addition to the discussion of simulated water masses and their overall favorable comparison to observations provided in the main text, several further descriptive aspects are detailed here.

The eastern open gyre (Fig. S1b) features two major water mass poles, the warm and salty warm deep waters (WDW) transiting along the modified warm deep water (MWDW) mixing lines into the fresher secondary pole of winter waters (WW) at the surface freezing point. The lighter Antarctic surface waters (AASW) though ccupying a large extent of the Θ-S_A space represent a comparatively small volume of ocean. Only a more modified version of the WDW pole makes it onto the eastern shelf to the south (Fig. S1f), where waters at the surface freezing point are the major water mass occupying a large range of salinities both fresh and also already somewhat salinified transiting in the range of dense shelf waters but remaining below 34.8 g/kg. A relatively small volume of subsurface freezing point waters is present, indicating the interaction with ice shelves (local, or upstream imported across the eastern boundary).

Moving westward onto the wide continental shelf in front of FRIS (Fig. S1e, repeated from Fig. 5), MWDW and WW still present major poles, and here a large fraction of the latter has

been salinified into a major pole of high salinity shelf waters (HSSW) with salinities in excess of 34.8 g/kg reaching peaks above 35.1 g/kg. Their interaction with FRIS produce fresher ice shelf waters (ISW) with temperatures below the surface freezing point, which upon leaving the cavity constitute a major water mass on the open continental shelf. On the continental shelf to the north adjacing the Antarctic peninsula (Fig. S1c), MWDW and WW are the major water masses, with salty HSSW present only in smaller quantities, and only a tiny fraction of ISW produced by the local interaction with Larsen ice shelves.

In the western open gyre (Fig. S1a) simulated water masses are overall similar to the eastern open gyre with major poles of WW and (M)WDW, but here a new water mass denser than MWDW is present occupying a large fraction of volume. This corresponds to Weddell sea deep and bottom waters (WSDW/WSBW) formed locally within the model domain through the simulated ocean–atmosphere–sea-ice interactions on the wide southern and western continental shelf and and ocean–ice-shelf interactions with the adjacent FRIS ice shelf. The eastern gyre (east of 25°W, Fig. S1b) only shows a small fraction of this water mass and only at its warmest extreme (with temperatures remaining above -0.5°C).

Cavity water masses Cavity water masses are color-shaded for the three ice-shelf cavity formations within the Weddell Sea regional domain: FRIS (Fig. 6), and EWIS (Fig. S2a) and Larsen (Fig. S2b). Whereas low volumes of AASW are found in each of the three cavities, the shallower Larsen and EWIS cavities, in contrast to the large and deep FRIS cavity, also show important volume fractions of MWDW. Whereas MWDW that enters Larsen is substantially modified and relatively cold ($\Theta < -1$°C), waters that reflect the characteristics of the major pole of WDW/MWDW in the eastern gyre and continental shelf regions are able to enter the EWIS cavities (up to 0°C). Together with substantial volumes of WW, these drive ice-shelf melting thereby transforming into ISW. Here ISW features several poles with different Θ-S_A properties in the different EWIS and Larsen cavities, being overall fresher in EWIS and saltier in Larsen.

Water-mass changes Fig. S3 provides a characterization of the impact of tides on regional water mass properties, by displaying the difference of oceanic volume in Θ-S_A space, between the reference simulation with tides and the perturbation experiment without tides. For lisibility across the large range of volumes and volume changes, instead of the simple difference, the Figure colors the difference of the logarithms of volume fractions weighted by the logarithm of the no-tide volume fractions, where the volume fraction is the ratio of the volume in

each Θ-S_A bin and the total ocean volume of the region considered. Characterization is provided for western & eastern open gyre (Fig. S3a & b), southwestern & eastern continental shelves (Fig. S3c & d), and FRIS & EWIS (Fig. S3e & f). Whereas tidally-induced water-mass changes are often small and fragmented, several key differences stand out as systematic and pronounced and have been highlighted in the main text. In particular, they consist, in the eastern Weddell Sea, in more sub-freezing-point water produced through larger melting in the EWIS cavities (Fig. S3f), which is accompanied with a slight enhancement of EWIS ISW on the eastern continental shelf outside (Fig. S3d). For the southwestern Weddell Sea, similar signatures of the tidally-driven enhancement of basal melt are seen: In the FRIS cavity (Fig. S3e), the volume of above-freezing-point waters diminishes while that of sub-freezing-point waters augments, with in the latter several poles of Θ-S_A changes with enhanced volume in particular in fresher FRIS ISW. On the southwestern continental shelf outside FRIS (Fig. S3c) outflowing ISW loose volume in their salty varieties but gain volume in their fresh varieties. Here also the saltiest waters along MWDW to HSSW/ISW mixing line decline, while the saltiest HSSW somewhat augment. Regarding the deep ocean beyond the continental shelves, while the eastern Weddell Sea (Fig. S3b) shows no substantial tidal impact, in the western open gyre (Fig. S3a) tides induce a marked change: here deep and bottom waters loose saltier and gain fresher varieties, as a consequence of the tidally-driven changes in ocean-cryosphere interactions in the southwestern Weddell shelf and cavity. Overall, as discussed in the main text, these provide evidence for an impact of the tidal enhancement of Weddell ice-shelf melting that, besides its consequence for ice shelves and adjacent ice sheets, extends beyond cavities: through the associated enhanced meltwater export it influences oceanic properties on the continental shelves, known for their generating role in the formation of Weddell Sea and global ocean deep and bottom waters.

Further differences in the Θ-S_A properties between the two experiments present throughout most of the 8-year simulations reflect tide-driven changes in the renewal of cavity water masses. Thus, in absence of tides, remote cavity localities exist, especially under FRIS, whose water masses are never fully flushed out. There (artificial) water masses present in the initial state, which themselves are remnants from the initialization of the forcing simulation (GO7) and thus survived a 14-year non-tidal spinup at coarser resolution (eORCA025), remain present throughout the 8-year no-tide perturbation experiment. To the contrary, in presence of tides, these are replaced by what are thought to be more physically-consistent FRIS cavity water masses within the first simulated year. In such remote cavity locations of lingering warm deep water masses,

inherited from extrapolated initial conditions, strong enhanced-melt anomalies may be expected. However, as in absence of tides water masses stagnate there, the tbl freshens and cools instead in response to the artificially concentrated meltwater in contact with the icedrafts. This is represented by small pockets of very fresh and cold water masses in the no-tide FRIS volumetric Θ-S_A that are too small in terms of volume to be visible on the color scale in Fig. S3. To provide further assessment of the impact of the differing renewal of these local cavity water masses on the net results presented in this study, a second sensitivity experiment has been realized. It makes use of the tidally-driven flushing out of water masses in the high-resolution tidally-forced reference experiment designed in this study, and removes tides from this tidal state at year 6 of the reference experiment for a two-year simulation. However, this second assessment strategy also cannot fully assess the impact of tides, as the no-tidal sensitivity simulation is not able to fully separate itself from its tidal-state initialization, and as suggested by present results, will likely not be able to do so for two decades or more. Whereas our analysis suggests that such local tide-induced phenomena do not contribute significantly to the integral tidal signatures discussed here, they nonetheless underline the important role of tides in shaping ocean–ice-shelf interactions and the renewal of water masses in large, deep and cold cavities such as FRIS.

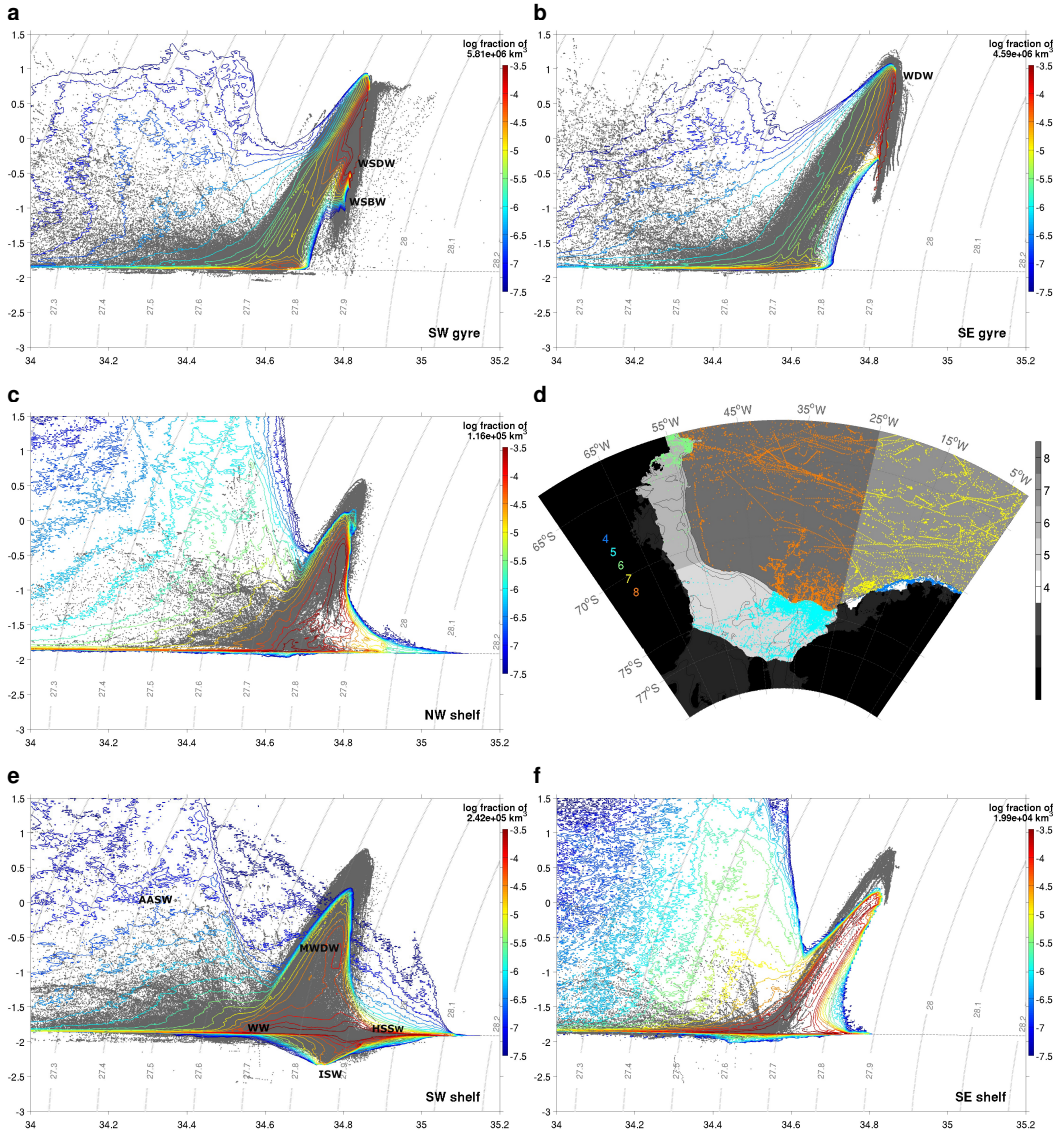

Figure S1. Further characterization of open-ocean water masses. Open-ocean regional subdomain (as mapped in **d**) volumetric Θ-S_A diagrams (colored contours, shown as log fraction of the respective region's total ocean volume) in the reference experiment (5-year average over years 4-8, i.e. 1993-1997). Dotted contours show σ_0. All-time available in-situ observations (mapped in **d**, one color per region, with numbers indicating region) are superimposed (as gray dots) over the regional model Θ-S_A diagrams. Regions displayed are: **a** the southwestern open gyre (n°8 in **d**), **b** the southeastern open gyre (n°7), **c** the northwestern Weddell shelf (n°6), **e** the southwestern Weddell shelf (repeated from the main text, n°5), and **f** the eastern Weddell shelf (n°4). Further water masses labelled, besides those indicated in the main text & panel **e**, are warm deep water (WDW) and Weddell Sea deep & bottom water (WSDW & WSBW).

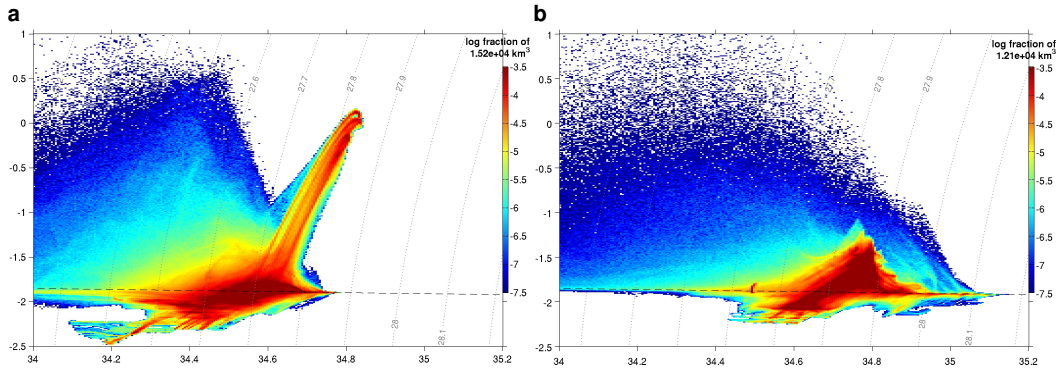

Figure S2. Further characterization of cavity water masses. Reference experiment 5-year average (years 4-8, i.e. 1993-1997) volumetric Θ-S_A diagram for the cavities of EWIS (**a**) and Larsen (**b**), shown as log fraction of the respective cavity's total ocean volume (colors). The corresponding water mass diagram for the FRIS cavity is displayed in the main text in comparison to sub-ice-shelf in-situ observations.

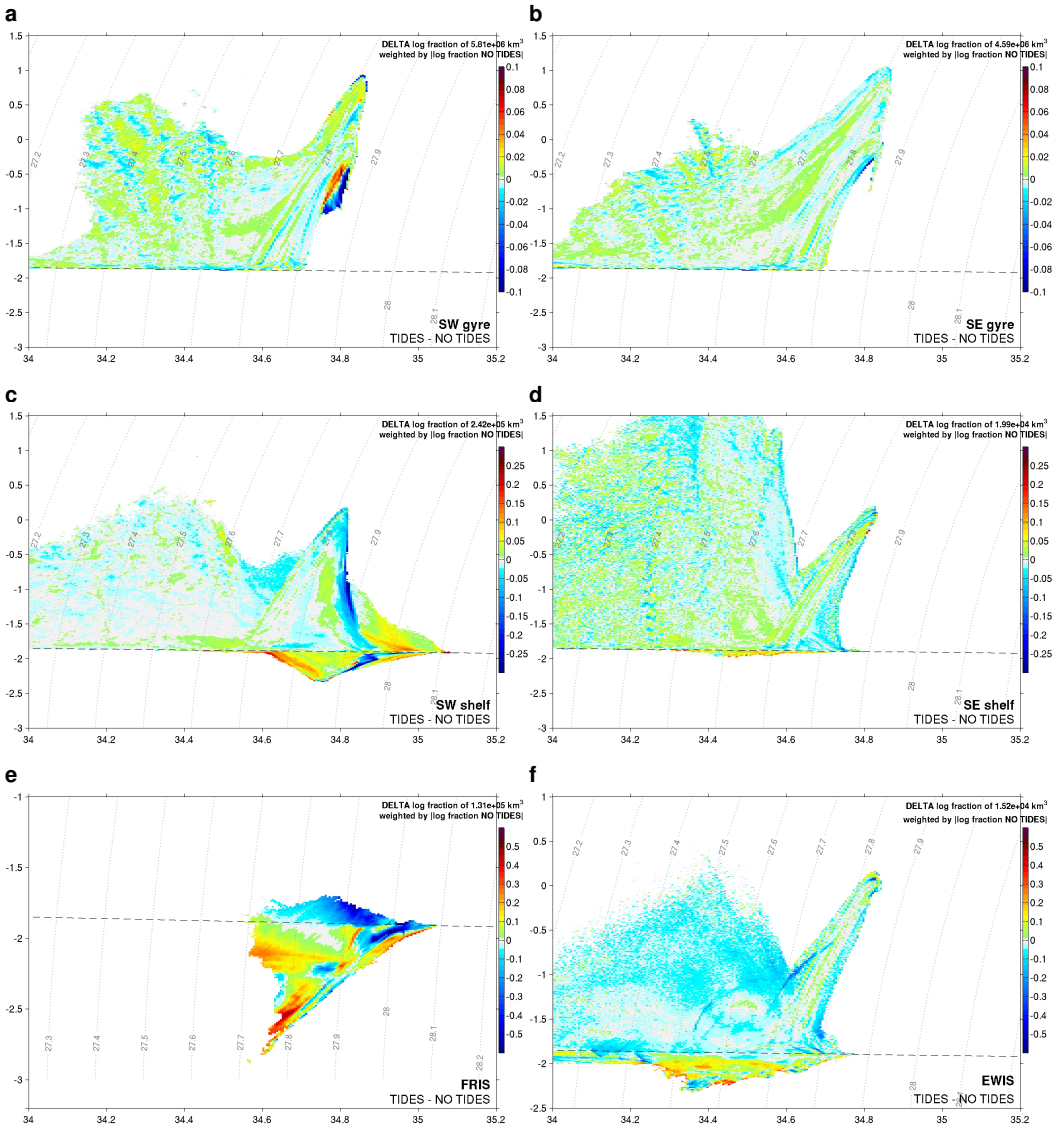

Figure S3. Impact of tides on water-mass properties, in the open ocean (cf. map locations in Fig. S1d) for **a** the southwestern & **b** the southeastern open gyre, **c** the southwestern & **d** the eastern continental shelves, and for the cavities of **e** FRIS & **f** EWIS. (For corresponding tidal reference Θ-S_A cf. Figs. 5, 6, S1 & S2.) Here, to visualize changes over the large magnitude range of ocean volumes concerned, panels display (in color) the ratio of Θ-S_A volume fractions (with respect to the total ocean volume of a given region V_0) in presence of to in absence of tides, weighted by the corresponding no-tide volume fraction, that is: $\left(log_{10}(\frac{V_{tide}}{V_0}) - log_{10}(\frac{V_{notide}}{V_0})\right) / \left|log_{10}(\frac{V_{notide}}{V_0})\right|$, colored only where both tide and no tide volume fractions exceed 10^{-7}. Thus, positive values (red shades) indicate a tidally-driven increase of volume in a given Θ-S_A bin, negative values (blue shades) a decrease. Values of $\pm.1$ indicate a change of volume by $n/10$ powers, where the volume without tides V_{notide} was $10^{-n}V_0$, and larger/smaller absolute values indicate larger/smaller relative changes. Note changing color bars, reflecting largest relative changes in cavities (lower panels), followed by continental shelves (middle) and then the open gyre (top).

Table S1. Ocean model parameterizations.[a]

free surface:	nonlinear, variable volume distributed through depth in time-varying z*-coordinate	(linear, fixed volume, with constant z-coordinate)
split-explicit free surface:	integrating barotropic equations with centered scheme	(forward scheme)
barotropic boundary conditions imposed via:	Flather radiation	(flow relaxation)
lateral momentum boundary condition via:	no slip	(partial slip)
nonlinear bottom & top friction, with drag:	varying with last ocean cell depth within 2.5e-3 & 1.e-2 (*Madec and NEMO-team*, 2016)	(constant value of 1.e-3)
vertical eddy diffusivity:	2.0e-6 m^2/s, modulated by horizontal shape function	(1.2e-5 m^2/s, without horizontal shape)
enhanced vertical diffusion:	10 m^2/s, applied on tracer	(tracer & momentum)

Notes: [a] Key ocean model parameterizations are as in Jourdain et al. 2017, besides those specifically listed here. In the table, parameterization choices used in this study are given in the middle column, and followed by Jourdain et al. 2017's choice (given in brackets in the last column). Configuration and experiment forcing strategies are detailed in the main text (sections 2.1 & 2.2), and in Jourdain et al. 2017, respectively. For further details of parameterizations employed refer to https://doi.org/10.5281/zenodo.3384022 for this study, and to https://doi.org/10.5281/zenodo.1067647 for Jourdain et al. 2017.